Water molecules in hydroxy/acid networks as a competition between dynamics and bonding. Synthesis of a wet hydrophobic pore

Natalia Pérez-Hernández,[a] Cirilo Pérez,[b,*] Matías L. Rodríguez,[b]
Concepción Foces-Foces,[c,*] Peter M. Tolstoy,[d] Hans H. Limbach,[d]
Ezequiel Q. Morales,[a] Ricardo Pérez[a] and Julio D. Martín[a,*]

[a]Instituto de Investigaciones Químicas, CSIC, Americo Vespucio, s/n, Isla de La Cartuja, 41092, Sevilla, Spain
[b]Instituto de Bioorgánica, Universidad de La Laguna, CSIC, Crta. Vieja de La Esperanza, 2, 38206 La Laguna, Tenerife, Spain
[c]Instituto de Química-Física Rocasolano, Departamento de Cristalografía, CSIC, Serrano 119, E-28006 Madrid, Spain
[d]Institut fuer Chemie der Freien Universitaet Berlin, Takustrasse 3, D-14195, Berlin, Germany

Abstract—In a model formed by hydroxy acids with a general structure (±)-**1**, we found that solid-state structures depend on steric interactions. Thus, with the exception of molecules **1b** and **1e**, compounds (±)-**1a**-(±)-**1m**, which possess bulky and conformationally rigid substituents, aggregate by forming tapes and sheets by alternating (+) and (−) subunits held together via carboxylic acid to alcohol hydrogen bonds. Homologue (±)-**1n** with conformationally flexible substituents, which allow conformational deformation gives, by way of the incorporation of water molecules, an efficient hexagonal assembly, which extends to the third-dimension to form tubular H-bonding networks. Each puckered channel can be described as being interconnected by closely packed hexagons in chair-like conformations. The ethyl groups presented in (±)-**1n** provided the volume required to lock the inner hexagonal wall into a rigid structure.
© 2003 Elsevier Ltd. All rights reserved.

1. Introduction

In biology, water and ions channels are molecular devices which facilitate large fluxes of water and ions across cell membranes in response to osmotic water regulation gradients[1] and electrical signals.[2] In such dynamic processes, the magnitude of the flux is strictly regulated by sophisticated designs of selection filters and conducting pathways, where a careful combination of hydrophobic and hydrophilic regions procure an isoenergetic environment which allow the efficient moving of ions, water or others small uncharged molecules across cell membranes. Thus, the way in which evolution has fine-tuned the amphipathic nature of the aquaporin-1[3] (AQP1) water channel has a key role in the rapid and reversible transport of water molecules, a property that is preserved along the large family of aquaporins.[1,4] Similarly, the non-polar water-filled cavity of the bacterial

KcsA K$^{\oplus}$ channel helps not only to overcome the dielectric barrier for potassium ions transport caused by the cell membrane,[5] but also constitutes the receptor site for the inactivation gate[6] and hydrophobic cation inhibitors.[7] However, many issues still await full comprehension. For example, how can the energy cost of the passage of water through the hydrophobic sections of a pore be saved?. One possibility could be that the water molecules arranged on the walls of the pore not be static, but rather in a dynamic exchange process, which would permit the permanent 'wetting' of the pore's interior. In other words, the hydrophobic configuration that results from static observation could be less so when (probable) dynamic processes of structural water diffusion are made to intervene procuring a continuous wetting path along the entire pore.

The internal radius of the water-filled hydrophobic cavity of KcsA K$^{\oplus}$ channel is about 5 Å; that of an aquaporin is, on average, 2 Å. However, the interpretation of these dynamic processes, which are based only on the static data that structural biology offer, is not straight-

* Corresponding author. Tel.: +95-448-9553; fax: +95-446-0665; e-mail: jdmartin@iiq.csic.es

forward, and complementary modelling studies are required to obtain a truly atomistic description of biological performance.[8,9] Thus, for example, a recent molecular dynamic simulation study that examines the behaviour of water within a (6, 6) carbon nanotube of 4.1 Å radius suggests that water molecules form H-bond chains that rapidly move through the tube in spurs.[10] This finding about hydrophobic pore wetting should be relevant for the mechanism of gating (opening and closing) of natural channels, and additional it is intrinsically important as a finding, since extends our general knowledge about water diffusion. Although much of the progress in this area come from theoretical studies,[11] complementary experimental efforts are doubtless needed.

2. Results and discussion

The hydrophobic effect[12] at aqueous biphasic systems influences not only the structure of the surface water but also the behavior of a wide variety of solutes in the interfacial region.[13] Simple considerations based on our knowledge of hydrophobicity at submolecular scale, lead to the expectation that equilibrium concentrations of small amphiphilic solutes should increase from both bulk phases to the interface, with their hydrophilic part exposed to the aqueous medium.[13,14] This equilibrium at the interface site induces ordered amphiphatic arrangements with consequences in the nucleation and packing of the solute molecules in the solid state.[15]

For a molecule that possesses axially oriented hydroxyl/carboxylic acid functions, the 'like-to-unlike' carboxylic acid-to-alcohol H-bonds was considered to be the most favorable arrangement in terms of energy, since pro-

curing an extended H-bonding array, oriented to the water subface at the time that the hydrophobic counterpart, remain immersed in the nonpolar subface (Fig. 1).

Based on this argument, we have reported[16] the synthesis of a new class of organic tubular material by selection, among the homologues of a family of general structure ($\pm$)-**1**, hydroxy/acids **1a–q** (Chart 1), the molecule with the optimized elements which achieve a hexameric cyclic assembly at the H_2O/CCl_4 interface, according to the course depicted in the Scheme 1. Of the sixteen homologues studied (Chart 1),[16b] only three: ($\pm$)-**1b**, **e** and **n**, provided 3-D networks by incorporation of water molecules, in the crystalline state. Two of these hydrated structures ($\pm$)-**1b**1/2H_2O and ($\pm$)-**1e**H_2O, derived from interdigitated single-stranded head-to-tail chains composed of pure enantiomers. The hexameric structure of ($\pm$)-**1n**·H_2O corresponds to the cyclic aggregate of a hydrated head-to-tail single-stranded chain made up of alternating (+)- and (−)-**1n** molecules (Scheme 1). The rest of compounds studied generated anhydrous packing composed of double-stranded head-to-tail arrays. These results demonstrate that when structurally robust H-bonded patterns are
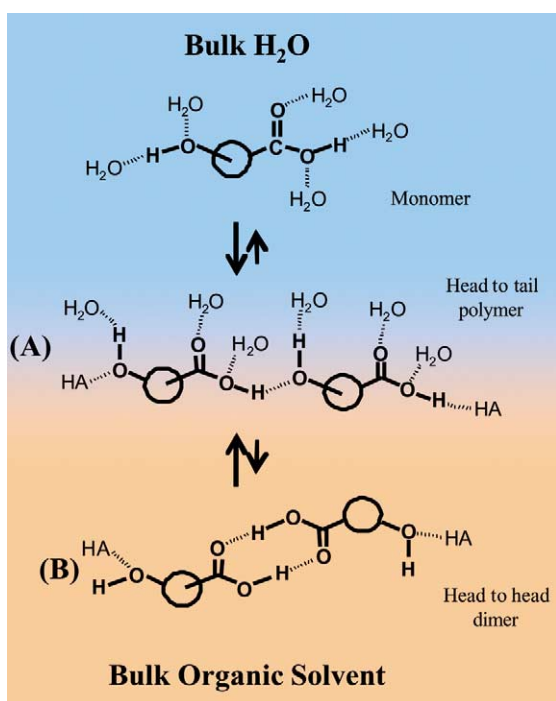

Figure 1. Schematic illustration of the equilibrium expected for an amphiphilic hydroxy/acid at the H_2O/organic solvent interface (A) and bulk nonpolar subface (B).
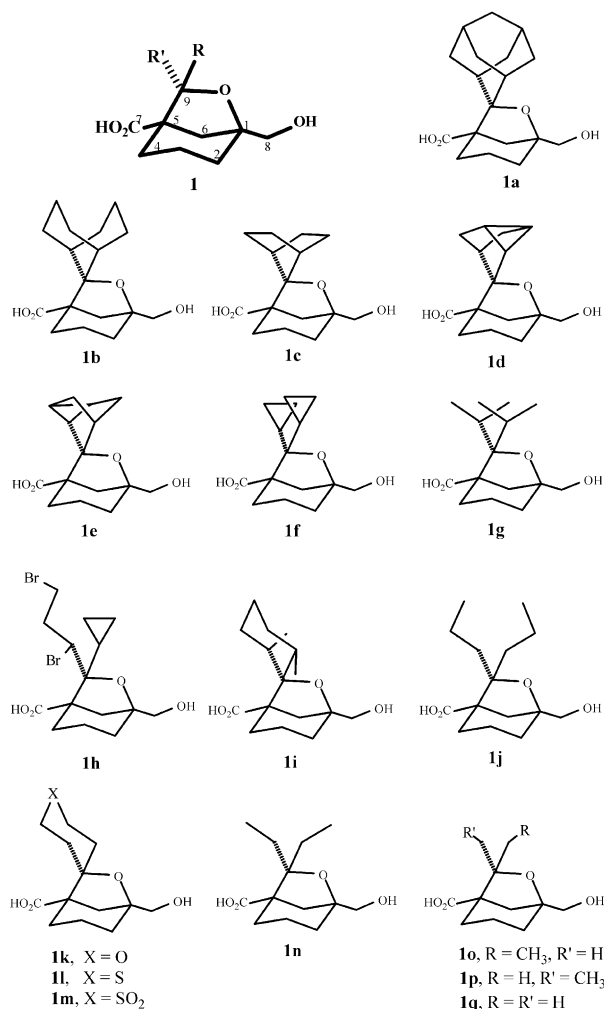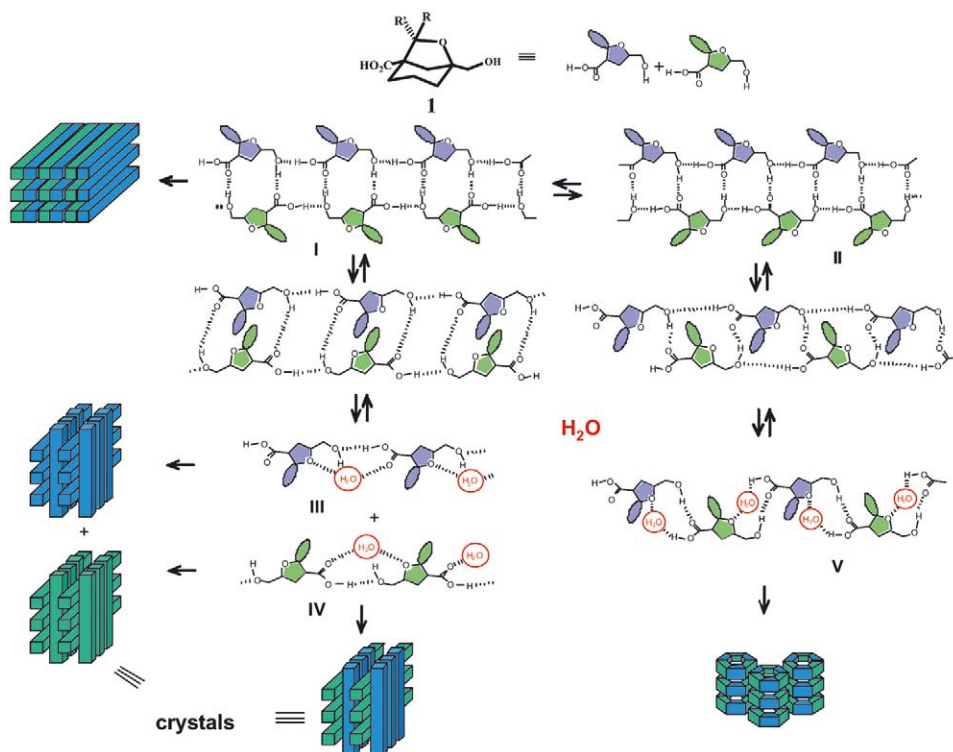

Chart 1.

Scheme 1. Schematic representation that illustrates the hydration and crystal growth processes of hydroxy acids of general structure (±)-**1** based on their anhydrous H-bonding pattern. It was expected the incorporation of water molecules into the double-stranded head-to-tail chains, I or II, will lead to hydrated single chains formed by unique enantiomers, III and IV, or alternating enantiomers, V, respectively. Thus, their packing expectation should depend on the course of the hydration equilibria.

employed, it is once more the combined steric requirements and the conformational flexibility of the substituents that govern which framework is adapted. We argue, at the same time, that the architecture of the target material can be reached by systematic changes in the size of monomers.

Crystals from all compounds were slowly grown under identical conditions using a previously water-saturated mixture of carbon tetrachloride/*n*-hexane as solvent. The structural organization present in the single-crystal study was shown to be representative of the bulk solid material structure by high resolution solid-state MAS-NMR spectroscopy.[17] Thus, the hexameric mono-hydrate (±)-**1**nH_2O converts to polymorphic anhydrous forms when conditions are altered due to its ability to lose water from hydration. When the monohydrate is placed in vacuum at 25 °C and ∼10^{-2} mbar for 24 h, the resulting material has a HMAS-NMR spectrum distinctly different from that of the monohydrate. Broader resonances arise from the presence of a significant amorphous phase in the sample. Although the stability of this amorphous anhydrate is not exactly known it is thought to crystallize very slowly and eventually reconvert to the monohydrate.[16b] Another form for compound (±)-**1n** that has been obtained as a pure phase is a crystalline anhydrate. This material was made via fast crystallization from the H_2O/CCl$_4$ interface and shown, by single-crystal X-ray study, to be made up of double-stranded enantiomorphic chains of (+)- and (−)-**1n** molecules joined in a head-to-tail fashion (Fig. 2a). This crystalline anhydrate is the most stable anhy-
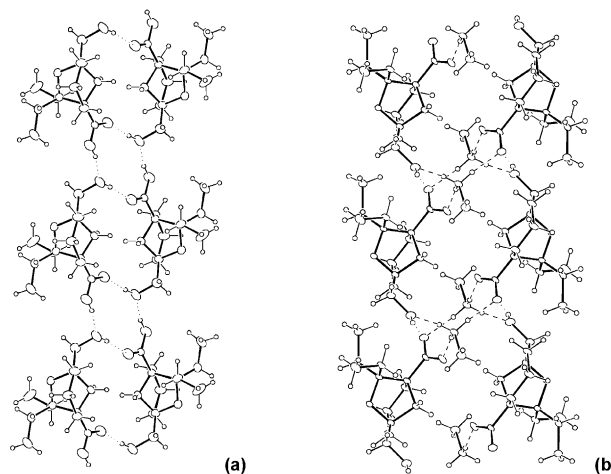

Figure 2. (a) Secondary structure of (±)-**1n** displaying a double-strand (1-D) network. (b) View of the 2-D network in (±)-**1n**MeNH$_2$ salt. The MeNH$_2$ molecules joins (+)- and (−)-**1n** molecules (dotted lines).

drous form when crystallization occurs in the absence of water,[16b] or at the H_2O/CCl$_4$ interface in the presence of methylamine. In the methylamine salt, the ammonium cations join molecules into double-stranded chains ($N^{+}...O^{-} = 2.725(3)$, $2.771(3)$ and $2.690(3)$ Å), in an also head-to-tail fashion (Fig. 2b) avoiding incorporation of water molecules. These strands are then assembled into layers by means of hydroxyl to carboxylate hydrogen bonds ($O...O^{-} = 2.697(3)$Å). All attempts to obtain amorphous or crystalline material including bulkier primary amines (ethyl-, *n*-propyl- or isopropyl-amine)

or diamines (1,3-diaminopropane or 1,4-diaminobutane) were unsuccessful. Albeit indirectly, these results demonstrate that the incorporation of water molecules into the H-bonding pattern to provide a hexameric structure, is sequential and follows the course depicted in the general Scheme 1.

Such behavior contrasts sharply with the preferences observed for this family of hydroxy/acids in the bulk organic solvent solution. We detail the next experiments based on ^{1}H NMR studies of compound (±)-**1n**, which demonstrate that in nonpolar solvent solutions, the compound dimerises preferentially through the carboxylic acid functions, forming a cyclic assembly.

The samples were prepared by dissolving a certain amount of the dried compound (±)-**1n** in CD_2Cl_2 and then preparing diluted samples by adding solvent. After plotting results of chemical shifts and line widths in dependence with temperature at four different concentrations, some trends have been identified for the signals belonging to the acid proton ($\delta = 12.5$ ppm) and the alcohol proton ($\delta = 2.5$ ppm). We began these series of experiments thinking that the line shape of these signals might give some information about the complexes eventually formed or preformed. For this purpose it was necessary to reach a considerable slow exchange regime, which was achieved by lowering the temperature. Signals could be observed below 213 K. Taking into account the acid proton signal and examining the behavior of the line width for a given concentration when lowering the temperature, it can be observed that at the highest temperature, where the signal first appears, the line is very broad (probably meaning there is still a dynamic exchange process taking place). At lower temperatures the line width begins to decrease and reaches a first minimum at 193 K, after that it begins to broaden again until the last temperature measured for some of the concentrations, 153 K (Fig. 3a). This behavior, first showing a sharpening of the line, then a broadening and again a sharpening which remains constant for all concentrations, is perhaps indicative that two separate dynamic processes are taking place. If the different concentrations are taken into account, for example comparing the line width at a certain temperature, some differences in the values are observed. However, it is difficult to assign a specific tendency when diluting the samples, because at some temperatures the most concentrated sample shows the broadest line (for example at 213 K or at 193 K) and at other temperatures it shows the sharpest (at 163 K or at 153 K). Another feature that is of some importance is that the differences in line width in relation to concentration decrease when lowering the temperature, even overlapping in some cases (i.e., 193 K and 163 K) (Fig. 3a).

When regarding the alcohol proton (Fig. 3b), the following features can be summarized: for a given concentration, the signal is broad at the higher temperature, starts to decrease when lowering the temperature and at a certain value begins to broaden again, until it finally disappears. Again it seems that a certain exchange is
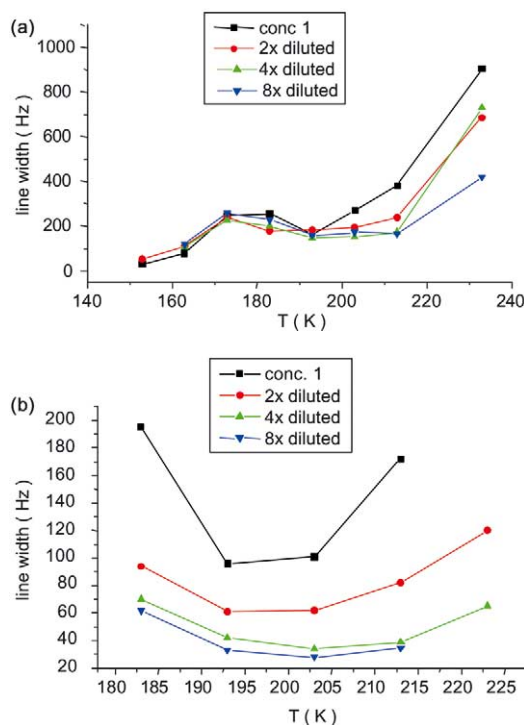

Figure 3. (a) Change when lowering temperature of the line width signal corresponding to the acid proton of **1n** in the ^{1}H NMR spectra. Initial concentration 23.5 mM solution in CD_2Cl_2. Serial of half-dilution. Concentrations: ■ 23.5 mM, ● 11.7 mM, ▲ 5.8 mM, ▼ 2.9 mM. (b) Change of the line width signal of the alcohol proton of **1n** when lowering the temperature.

slowed down at the beginning, and then another one starts to be fast enough to cause a broadening of the signal. This behavior is consistent for the range of studied concentrations, although the individual values of the line widths for each concentration become smaller with dilution. In contrast with the acid proton, there is no overlapping and only the last two concentrations values become closer. There is, therefore, a dependence on the line width in relation to concentration in this particular case.

The minimum of line broadness for the alcohol proton signal is found at 193 K for the two more concentrated samples and at 203 K for the both less concentrated ones. In the case of the acid proton the first sharpening occurs at 193 K for three of the concentrations and at 183 K for the remaining one (Fig. 3a). This could suggest that, at these temperatures, both protons are taking part in an exchange process that is slow down, and when the temperature decreases 'diverge' and experiment different dynamic processes. In any case, it seems that for the acid proton, this other process is also being slowed when lowering the temperature below 173 K.

If we focus on the chemical shift, there is a general feature common to both signals: as temperature decreases, the chemical shifts increases, that is, the signal appears at lower field. If both protons are involved in hydrogen bond bridges, this could be consistent with the theory that the number of hydrogen bonds increases when lowering temperature (Fig. 4a,b).
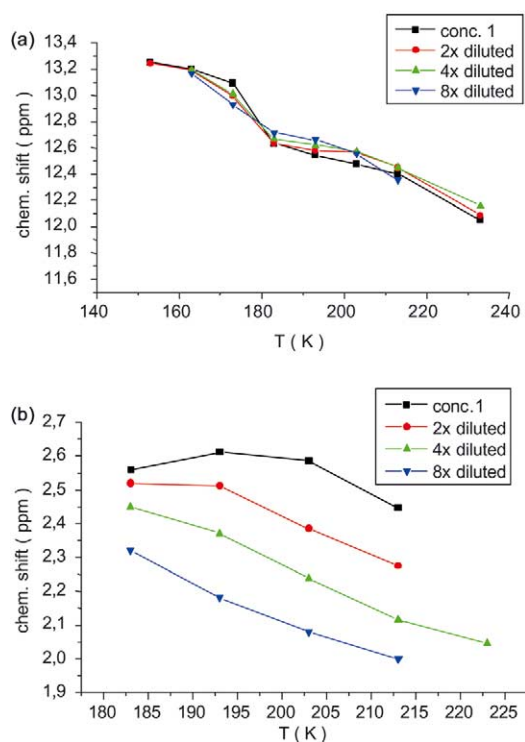
Figure 4. (a) Change when lowering temperature of the chemical shift of the acid proton of **1n** in the ^{1}H NMR spectra. Serial of half-dilution under the same conditions as given in Figure 3. (b) Change of the chemical shift of the alcohol proton signal of **1n** when lowering the temperature. Concentrations: ▬■▬ 23.5 mM, ▬●▬ 11.7 mM, ▬▲▬ 5.8 mM, ▬▼▬ 2.9 mM.

When only taking into account the acid proton signal, it is not possible to establish certain trends when changing concentrations. For a given temperature, the values of the shifts are quite close to each other and do not always follow a sequence; for example, at 193 K the most concentrated sample is the one with the smallest chemical shift and the most diluted sample is the one with biggest chemical shift, this is exactly the opposite at 173 K. Maybe it would be possible to say that the increase in chemical shift takes place in a smoother way for the more diluted samples; in fact, the largest difference between two adjacent values is found for the more concentrated sample at 183 K and 173 K (Fig. 4a).

When examining the alcohol proton signal, a somewhat striking feature is that the two more concentrated samples, even following the general rule of increasing the chemical shift when lowering temperature, have an abrupt stop in this increase at the lowest temperature measured. Observing the graph (Fig. 4b), one can see that the slopes of the first two lines decrease and in the case of the most concentrated sample, it even becomes negative, as if the chemical shift would first increase and then decrease. When the dependence of the chemical shift regarding concentration is examined, a very clear tendency is observed: the more diluted the samples are, the smaller the chemical shift is. That is to say, for a given temperature, the less concentrated samples show a signal at a higher field. The lines that bind the points for each concentration never overlap, so the differences can be clearly observed.

After this description of line width and chemical shift behavior values in relation to temperature and concentration, the first generalized feature can be emphasized: the tendencies in both parameters show clear differences when examining both the acid and the alcohol signals. This difference can be briefly described as a dependence of the line width and chemical shift on the concentration in the case of the alcohol proton signal, and the corresponding non-dependence in the case of the acid proton signal. This might suggest that, at low temperatures, some associations are formed that involve these two functions in different ways. Perhaps a coherent suggestion is the formation of cyclic dimers or trimers involving hydrogen bridges between carboxylic functions keeping the alcohol groups free. Under temperatures low enough to make these eventual lifetime associations long enough to be observed, the non-dependence of the chemical shift of the acid proton signal with relation to concentration could be explained as the hydrogen bonds between carboxylic acids should not be significantly affected by the presence of greater or lesser number of molecules.

On the other hand, the 'free' hydroxyl groups may, at the same temperatures, have the possibility of forming weaker hydrogen bonds to other OH groups and their existence could be affected by concentration levels. When these 'free' OH are able to meet a large number of other 'free' OH in their surroundings, the number of H-bonds formed between them will be higher, and the other way around. This would explain why the alcohol proton signal shifts to a higher field when the concentration is lowered. The number of H-bonds involving this alcohol proton would decrease, thus leading to the proton to stay closer to the oxygen and therefore more shielded. The shift to a lower field when temperature is decreased can be explained, as mentioned above, by an increasing of the H-bond number in both cases.

However, although the line width dependence on concentration suggests the presence of a structure where the carboxylic acid and the alcohol are involved in various H-bonded assemblies, the subsequent broadening and sharpening of the signals remain unexplained. The general sharpening of the signals when lowering concentration of the alcohol proton signal could mean an increase in the lifetime of some associations, perhaps because of a slow down in the molecular exchange in the more diluted samples. Trying to explain the trends at the lower temperature, where the lines become broader, in accordance with the hypothesis expressed above, it would seem that the proton exchange between alcohol groups of different associations is not being slowed enough at the temperatures measured. It is also important to mention that when diluting the samples by adding solvent, traces of water dissolved in the CD_2Cl_2 were being added at the same time. The exchange that seems to take place involving the alcohol group could also involve this water, although the temperatures are low enough to expect the water to be already frozen. In addition, the behavior of the acid proton signal line width remains unclear.

As a continuation of this study, we investigated the ^{1}H NMR spectra of a series of diastereomeric salts prepared

from compounds of general structure (±)-**1** (**1a–q**) and L-(−)-α-methylbenzylamine in CDCl$_3$. With no exceptions, it was found that these salts form diastereomeric dynamic systems the ^{1}H NMR spectra of which show typical anisochronism of the diastereotopic hydroxymethyl protons. This is due to the fact that in nonpolar solvents, particularly in those having weak ionizing properties, the disteriomeric salts exist according to the following equilibrium (eq. 1):
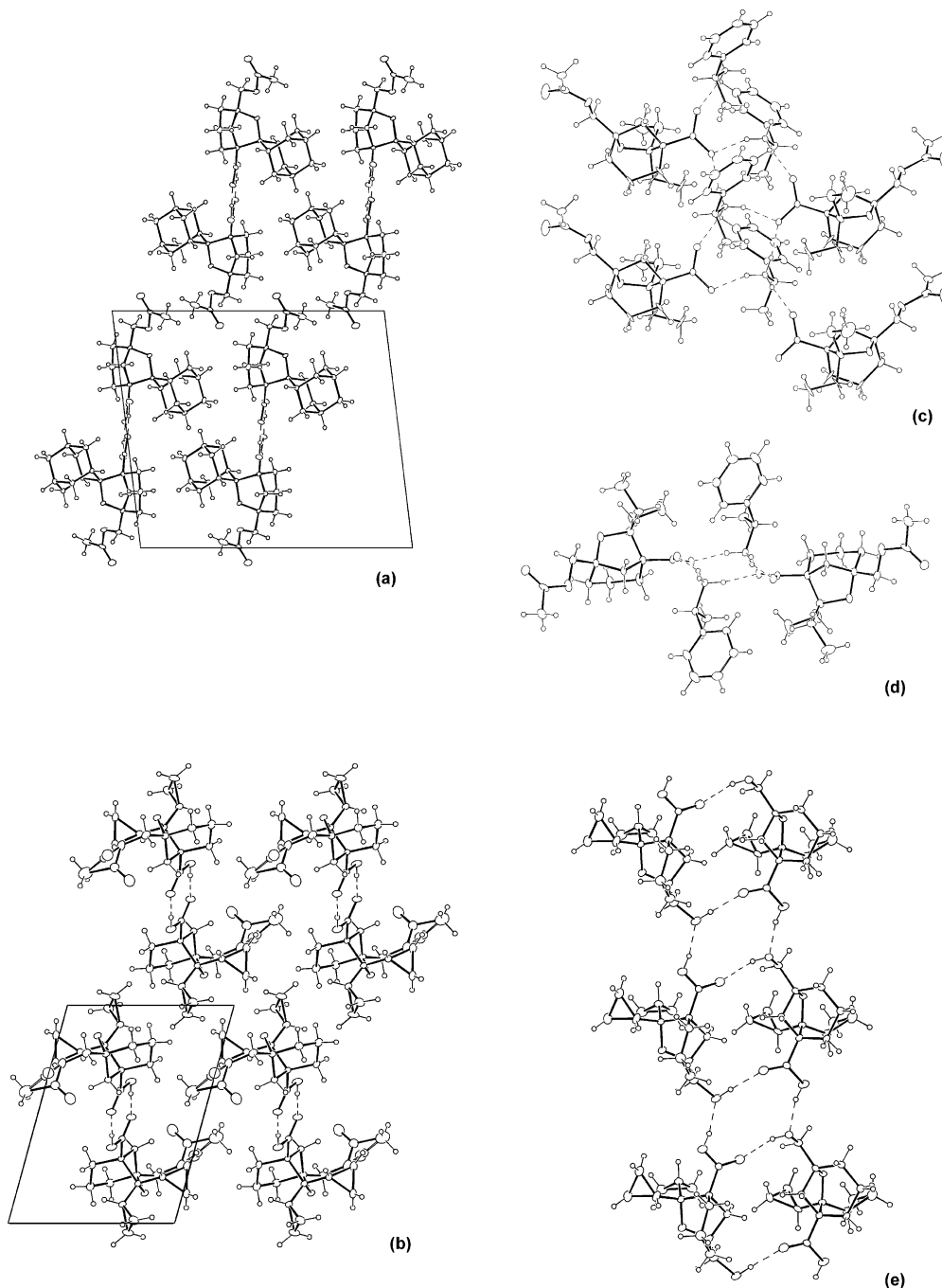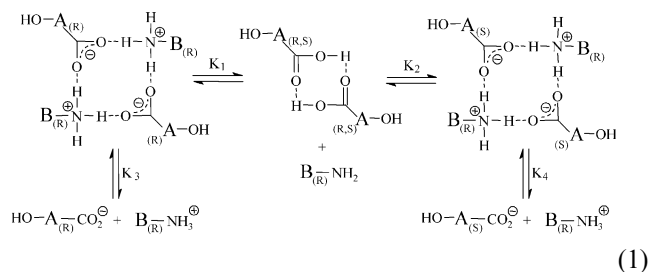
$$(1)$$

Figure 5. (a) Crystal packing of (±)-**1a**. (b) Crystal packing of (±)-**1f**. (c,d) Two views of the 1-D network in the L(−)-α-methylbenzylamine/(−)-**1n** (monoacetate) salt. (e) 1-D network of (−)-**1f**.

Free enantiomeric acids, or cyclic dimers, and free optically active bases, as well as the completely dissociated components; i.e., enantiomeric anions and ammonium cations, cannot cause non-equivalence. It can be caused only by the non-dissociated forms of the salt, the existence of which in the form of ion aggregates is favored by nonpolar solvent and low temperatures.

In agreement with these observations, Figures 5a and b show the crystal structures of monoacetates (±)-**1a** and (±)-**1f**, which consist of dimers formed by the assembly of both enantiomers around inversion centers via the carboxylic acid groups (O...O distances, 2.654(2) and 2.631(2)Å). Figures 5c and d, show the structure of the diastereomeric salt pair: L(−)-α-methylbenzylamine/(−)-**1n** (monoacetate). There are no independent ion pairs consisting of one acid molecule and one base molecule linked to one another. In the diastereomer presented, each ammonium group is short linked to three oxygen atoms through equivalent hydrogen bonds (2.786(5), 2.880(5) and 2.725(5) Å). In the salt, columns formed from four ions (two acids and two bases, Fig. 5d) are wrapped around helical 2_1 axes. Two types of intermolecular interactions are thus distinguished: strong hydrogen bonds, which form the molecular column, and weak van der Waals interactions between columns, which are responsible for the cohesion of the packing. Pure (−)-**1n** enantiomer[18] results to be an oily, non-crystalline substance. However, application of same protocol to the resolution of (±)-**1f** homologue gave pure (−)-**1f**, which crystallizes from H_2O/CCl_4 similarly to what happened with its racemic mixture,[16b] that is, forming double-stranded head to tail chains (Fig. 5e). These selected results, which are general for all the homologues studied, demonstrate that in bulk nonpolar organic solutions the dimeric H-bonding assemblies, among carboxylic acids, rule the nucleation and crystal growth and allow, in contrast to what was observed at
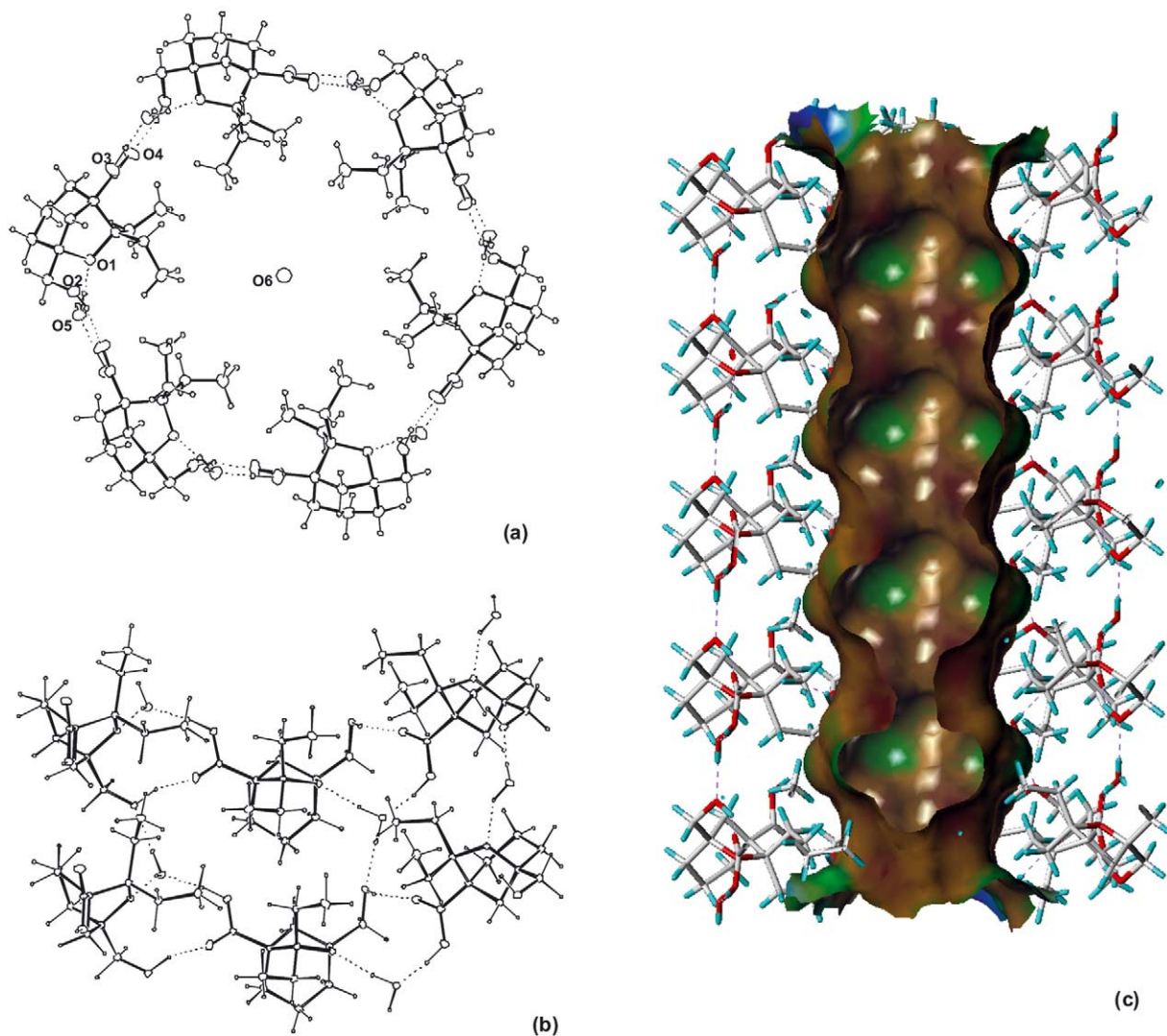

Figure 6. (a) Hexameric association of (±)-1n**æ** H_2O down the three-fold inversion axis. (b) Partial packing of two hexameric units (three molecules on each) showing the water molecules environment involved in the cohesion of the tubular structure. (c) Inner Conolly surface[19] through the channel with lipophilic potential mapped on to it. Z-axis clipping is done to observe the surface clearly.

the H_2O/CCl_4 interface, the smooth insertion of primary amines in their H-bonding array.

2.1. Hydrophobic tubular structure

The structure of (±)-**1n**H_2O is dominated by a hexameric ring of alternating (+)- and (−)-1n molecules held together by O2-H2···O4 H-bonds (Fig. 6a). This ring system, which is the striking feature of this molecular assembly, joins by c translation to another one via hydrogen bonds involving six water molecules, each one using one of its hydrogen atoms for that link to O2. Moreover, they act as donors of another hydrogen bond to O1 and accept a strong hydrogen bond from O3, which reinforces the ring system. The rings stack in this way to give columns defining c axis (Fig. 6b), all through the crystal, creating a pore, which holds disordered water molecules. The interior surface characteristics of the channels alternate between the hydrophobic domains created by the ethyl moieties, and the more hydrophilic interior at the ring-stacking sites (Fig. 6c). Nonstructural water molecules near the hydrophobic domains are considerably more disordered, displaying only a weak residual electron density. A disordered water molecule (O6) was located on a 3-fold inversion axis (Fig. 6a) and was allowed to refine up to a site-occupancy factor of 0.20 (6) and isotropic thermal vibration. The maximum positive peak in the final difference map (0.91 e $Å^{-3}$) occurs in positions close to the O6 molecule (1.67 Å) that could be considered as possible alternative locations for the O6 molecule although it was impossible to refine.[16a] Thus, the observed electron density for water (O6) is the time-average of water molecules binding at several overlapping sites, which suggest a facile movement of loosely held water molecules within the cavity. In the extended nanotube structures, the electron density forms a discontinuous wetting path through the entire pore.

The proven stability of hydrated cyclic aggregates from the optimised homologue (±)-**1n**, suggests that such a supramolecular structure might also reasonably be found in a lipid membrane environment. Thus, at the water-membrane interface, compound (±)-**1n** is expected to aggregate as in aqueous biphasic systems; that is, the hydrophilic face of the ring buried in water while the hydrophobic face remain exposed to the nonpolar environment formed by the hydrocarbon lipids tails. The expected hydrophobic tubular structure by ring stacking should insert into the membrane in a parallel direction to the lipid molecules. This suggestion, which is reinforced by the ionophoric activity shown by (±)-**1n** in phospholipid bilayers,[16a] is, however, tentative and thus requires further investigation.

Obviously, if the observed solid-state structure for (±)-**1n** is formed in a bilayer, the predominantly hydrophobic water-filled pore should contribute to the stabilization of ions. Because its inside is lined with hydrophobic ethyl chains, it is unlikely that a permeant ion will shed its hydration shell. Then, it would be interesting to know if such a simple model could overcome the dielectric barrier presented by the membrane, providing a water-filled pathway that allows passive flux of hydrated cations through the central and mostly hydrophobic pore.[20]

3. Conclusions

Much dynamic takes place in organic crystals at room temperature.[21] The reversion of these associations allows a continuous change in its constitution by internal molecular rearrangements or by exchange, incorporation, and extrusion of components. This model shows that the addition of water molecules displaces the dynamic equilibrium toward the preferential formation of the optimum H-bonding pattern, in a target-driven selection of the fittest.

This paper also tries to show that the application of general thermodynamic principles can predict the overall hydration behavior of a family of compounds. It is impossible, however, to unmistakably link the behavior of a particular homologue with a pre-defined crystalline state in advance and its need to be optimised from a family of homologues. This example illustrates how the assembly of hydrophobic structures requires the removal of water molecules from their H-bonding pattern in terms of enthalpy/entropy compensation. The generalization drawn from here might have relevance to the noncovalent complexes that are involved in certain biological functions. Finally, this model suggests that resolving the uncertainty of the incorporation of water molecules into organic H-bonding arrays requires the solution of a *cause/effect*[22] (molecular recognition) problem, that is, finding the best symmetric arrangement pattern for the optimum close-packing.

4. Experimental

4.1. X-ray crystallography

Crystal data were collected using a Nonius Kappa CCD diffractometer (λ(MoKa) = 0.7107Å) equiped with an Oxford Cryosystem cryostream. Data for (±)-**1n**MeNH₂, L(−)-α-methylbenzylamine/(−)-1n monoacetate, (−)-**1f**, and (S)-1-phenylethan-1-yl-(S)-phenylethan-1-yl-carbonate were collected at 170K whereas data for (±)-**1a** and (±)-**1f** monoacetates were recorded at 149 K. Data reduction and cell refinement were carried out with the programs DENZO[23] and COLLECT.[24] The structures were solved by direct methods[25] and the refinement process has been carried on F^2 against all data using SHELX97.[26] Detailed crystal data and geometrical parameters are deposited in the Supporting Information (CIF files).[27]

References and notes

1. (a) Preston, G. M.; Piazza-Carroll, P.; Guggino, W. B.; Agre, P. *Science* **1992**, *256*, 385. (b) Agre, P.; Bonhivers, M.; Borgnia, M. J. *J. Biol. Chem.* **1998**, *273*, 14659.

2. (a) Hille, B. *Ionic Channels of Excitable Membranes, Sinauer*, 2nd edn; Sutherland: M, 1992. (b) Moczydlowski, E. *Chem. Biol.* **1998**, *R291*. (c) Hucho, F.; Weise, C. *Angew. Chem. Int. Ed.* **2001**, *40*, 3100.

3. Sui, H.; Han, B.; Lee, J. K.; Walian, P.; Jap, B. K. *Nature* **2001**, *414*, 872.

4. (a) Ishibashi, K.; Kuwahara, M.; Gu, Y.; Tanaka, Y.; Marumo, F.; Sasaki, S. *Biochem. Biophys. Res. Commun.* **1998**, *244*, 268. (b) Meinild, A. K.; Klaerke, D. A.; Zeuthen, T. *J. Biol. Chem.* **1998**, *273*, 32446. (c) Borgnia, M.; Nielsen, S.; Engel, A.; Agre, P. *Annu. Rev. Biochem.* **1999**, *68*, 425. (d) Sui, H. S.; Han, B.-G.; Lee, J. K.; Walian, P.; Jap, B. K. *Nature* **2001**, *414*, 872. (e) Groot, B. L.; Grubmüller, H. *Science* **2001**, *294*, 2353. (f) Borgnia, M. J.; Agre, P. *Proc. Natl. Acad. Sci. U.S.A.* **2001**, *98*, 2888.

5. (a) Doyle, D. A.; Morais-Cabral, J.; Pfuetzner, R. A.; Kuo, A.; Gulbis, M.; Cohen, S. L.; Chait, B. T.; Mackinnon, R. *Science* **1998**, *280*, 69. (b) Jiang, Y.; Mackinnon, R. *Science* **1998**, *280*, 69. (c) Morais-Cabral, J. H.; Zhou, Y.; Mackinnon, R. *Nature* **2001**, *414*, 37. (d) Zhou, Y.; Morais-Cabral, J. H.; Kaufman, A.; Mackinnon, R. *Nature* **2001**, *414*, 43. (e) Yellen, G. *Nature* **2002**, *419*, 35.

6. (a) Perozo, E.; Cortes, D. M.; Cuello, L. G. *Science* **1999**, *285*, 73. (b) Zhou, Y.; Morais-Cabral, J. H.; Mann, S.; Mackinnon, R. *Nature* **2001**, *414*, 657.

7. (a) Cook, N. S. *Trends Pharmacol. Sci.* **1988**, *9*, 21. (b) Robertson, D. N.; Steinberg, M. I. *J. Med. Chem.* **1990**, *33*, 1529. (c) Blaustein, R. O.; Cole, P. A.; Williams, C.; Miller, C. *Nat. Struct. Biol.* **2000**, *7*, 309. (d) del Camino, D.; Holmgren, M.; Liu, Y.; Yellen, G. *Nature* **2000**, *403*, 321. (e) Luzhkov, V.B; Åqvist, J. *J. FEBS Letters* **2001**, *495*, 191.

8. For MD simulation studies on the basis of the X-ray structure of AQP1 and GlpF, see: Tajkhorshid, E.; Nollert, P.; Jensen, M.; Miercke, L. J. W.; O'Connell, J.; Stroud, R. M.; Schulten, K. *Science* **2002**, *296*, 525.

9. (a) For M.D. simulation studies on the basis of the X-ray structure of the KcsA K.$^{\oplus}$ channel[5]: Roux, B.; Mackinnon, R. *Science* **1999**, *285*, 100. (b) Berneche, S.; Roux, B. *Nature* **2001**, *414*, 73.

10. Hummer, G.; Rasaiah, J. C.; Noworyta, J. P. *Nature* **2001**, *414*, 188.

11. (a) In particular, a number of model studies have employed molecular dinamics to simulate the behavior of water molecules between two planar hydrophobic surfaces, spherical hydrophobic pockets or channel-like cavities Belch, A. C.; Berkowitz, M. *Chem. Phys. Lett.* **1985**, *113*, 278. (b) Rossky, P. J.; Lee, S. H. *Chem. Scr.* **1989**, *29A*, 93. (c) Walqvist, A.; Berne, B. J. *J. Phys. Chem.* **1995**, *99*, 2893. (d) Sansom, M. S. P.; Kerr, I. D.; Breed, J.; Sankararamakrishnan, R. *Biophys. J.* **1996**, *70*, 693. (e) Lum, K.; Luzar, A. *Phys. Rev.* **1997**, *E56*, R6283. (f) Lum, K.; Chandler, D.; Weeks, J. D.; Weeks, J. D. *J. Phys. Chem. B* **1999**, *103*, 4570. (g) Gelb, L. D.; Gubbins, K. E.; Radhakrishnan, R.; Sliwinska-Bartkowiak, M. *Rep. Prog. Phys.* **1999**, *62*, 1573. (h) Bolhuis, P. G.; Chandler, D. *J. Chem. Phys.* **2000**, *113*, 8154. (i) Sansom, M. S. P.; Shrivastaka, I. H.; Ranatunga, K. M.; Smith, G. R. *Trends Biochem. Sci.* **2000**, *25*, 368. (j) Hummer, G.; Rasaiah, J. C.; Noworyta, J. P. *Nature* **2001**, *414*, 188. (k) Koga, K.; Gao, G. T.; Tanaka, H.; Zeng, X. C. *Nature* **2001**, *412*, 802.

12. (a) Kauzmann, W. *Adv. Prot. Chem.* **1959**, *14*, 1. (b) Franks, F. *Faraday Symp. Chem. Soc.* **1982**, *17*, 7. For a recent view of this concept, see: Chandler, D. *Nature* **2002**, *417*, 491.

13. Pratt, L. R.; Pohorille, A. *Chem. Rev.* **2002**, *102*, 2671.

14. (a) Pratt, L. R. *Annu. Rev. Phys. Chem.* **2002**, *53*, 409 -. (b) Blokzijl, W.; Engberts, J. B. F. N. *Angew. Chem. Int. Ed.* **1993**, *32*, 1545.

15. Kuzmenko, I.; Rapaport, A.; Kjaer, K.; Als-Nielsen, J.; Weissbuch, I.; Lahav, M.; Leiserowitz, L. *Chem. Rev.* **2001**, *101*, 1659.

16. (a) Pérez, C.; Espínola, C. G.; Foces-Foces, C.; Núñez-Coello, P.; Carrasco, H.; Martín, J. D. *Org. Lett.* **2000**, *2*, 1185. (b) Carrasco, H.; Foces-Foces, C.; Pérez, C.; Rodríguez, M. L.; Martín, J. D. *J. Am. Chem. Soc.* **2001**, *123*, 11970.

17. (a) Solid-state NMR spectroscopy is a powerful method for investigating polymorphism in organic materials. Recent selected examples are: Harper, J. K.; Facelli, J. C.; Barich, D. H.; McGeorge, G.; Mulgrew, A. E.; Grant, D. M. *J. Am. Chem. Soc.* **2002**, *124*, 10589. (b) Harper, J. K.; Grant, D. M. *J. Am. Chem. Soc.* **2000**, *122*, 3708. (c) Zell, M. T.; Padden, B. E.; Grant, D. J. M.; Schroeder, S. A.; Wachholder, K. L.; Prakash, I.; Nunson, E. J. *Tetrahedron* **2000**, *56*, 6603. (d) Smith, J.; Macnamara, E.; Raftery, D.; Borchard, T.; Byrn, S. *J. Am. Chem. Soc.* **1998**, *120*, 11710. (e) Zell, M. T.; Padden, B. E.; Grant, D. J. W.; Chapeau, M. C.; Prakash, I.; Munson, E. J. *J. Am. Chem. Soc.* **1999**, *121*, 1372.

18. Most interesting, when the diastereomeric salt of L(−)-α-methyl-benzylamine/(−)-**1n** (monoacetate) was refluxed with potassium carbonate in acetone gave, after extraction, (−)-**1n** and diester carbonate of (S*)-1-phenylethan-1-ol by substitution at the carbon wearing the amine. The structure of this diester was determined to be homochiral by a single-crystal X-ray study. To the best of our knowledge (CSD 2002 release: Allen, F. H.; Davies, J. E.; Galloy, J. J.; Johnson, O.; Kennard, O.; Macrae, C. F.; Mitchell, E. M.; Mitchell, J. F.; Smith, J. F.; Watson. D. G. *J. Chem. Info. Comput. Sci.* **1991**, *31*, 187–204) only the synthesis of the R, S-isomer has been previouly reported: Pozo, M.; Gotor, V. *Tet. Asymm.* **1995**, 2797.

19. Done with MOLCAD module of Sybyl® 6.8 Tripos inc.; 1699 South Hanley Rd.; St Louis, Missouri, 63144, USA.

20. (a) For recent and selected examples related with synthetic channels and pores, see: Gokel, G. W.; Murillo, O. *Acc. Chem. Res.* **1996**, *29*, 425. (b) Fyles, T.M.; van Straaten-Nijenhuis, W.F. in *Comprehensive Supramolecular Chemistry*, Reinhoudt, D.M. Ed.; Elsevier Science Ltd.; Oxford, **1996**; Vol 10, p 53 (c) Voyer, N. *Top. Curr. Chem.* **1996**, *184*, 1. (d) Meillon, J.-C.; Voyer, N. *Angew. Chem. Int. Ed.* **1997**, *36*, 967. (e) Hartgerink, J. D.; Clark, T. D.; Ghadiri, M. R. *Chem. Eur.* **1998**, *4*, 1367. (f) Gokel, G. W. *Chem. Commun.* **2000**, 1. (g) Bayley, H. *Curr. Opin. Biotechnol.* **1999**, *10*, 94. (h) Bong, D. T.; Clark, T. D.; Granja, J. R.; Ghadiri, M. R. *Angew. Chem. Int. Ed.* **2001**, *40*, 988. (i) Goto, C.; Yamamura, M.; Stake, A.; Kobuke, Y. *J. Am. Chem. Soc.* **2001**, *123*, 12152. (j) Leevy, W. M.; Donato, G. M.; Ferdani, R.; Goldman, W. E.; Schlesinger, P. H.; Gokel, G. M. *J. Am. Chem. Soc.* **2002**, *124*, 9022.

21. (a) Gavezzotti, A. *J. Mol. Struct.* **1999**, *486*, 485. (b) Gavezzotti, A. *J. Mol. Struct.* **2000**, *615*, 5.

22. The oldest reference of this concept, applied to the solid state, might be: Curie, P. *J. Phys. (Paris)* **1894**, *3*, 393.

For a recent reference: Orme, C. A.; Noy, A.; Wierzbicki, A.; McBride, M. T.; Grantham, M.; Teng, H. H.; Dove, P. M.; De Yoreo, J. J. *Nature* **2001**, *411*, 775.

23. Otwinowsky, Z.; Minor, W. *Methods in Enzymology, Macromolecular Crystallography. Part A*, Carter, C. E.; Sweet, R.M. Eds.: Academic Press; University of Texas, Southwestern Medical Centre at Dallas, HKL DENZO and Scalepack, USA. 1997, Vol. 276, 307.

24. (COLLECT). Nonius, 1998. KappaCCD Server Software. Nonius B.V, Delft. The Netherland.

25. Altomare, A.; Burla, M. C.; Camalli, M.; Cascarano, G.; Giacovazzo, C.; Guagliardi, A.; Moliterni, A. G. G.; Polidori, G.; Spagna, R. *SIR97. J. Appl. Cryst* **1999**, *32*, 115.

26. Sheldrick, G.M. SHELXL97. University of Gottingen, Germany, 1997.

27. Crystallographic data (excluding structure factors) for the structures in this paper have been deposited with the Cambridge Crystallographic Data Centre as supplemtary publication nos. CCDC 198770-198775 for (±)-**1n**MeNH$_2$, L(−)-α-methylbenzylamine/(−)-**1n** (monoacetate), pure (−)-**1f** enantiomer, diester carbonate of (S*)-1-phenylethan-1-ol, monoacetates (±)-**1a** and (±)-**1f**, respectively. Copies of the data can be obtained, free of charge, on application to CCDC, 12 Union Road, Cambridge CB2 1EZ, UK (fax: +44-1223-336033 or e-mail: deposit@ccdc.cam.ac.uk).